Simulation studies of pressure and density wave propagations in vertically vibrated beds of granules

Keiko M. Aoki and Tetsuo Akiyama
Faculty of Engineering, Shizuoka University, 3-5-1 Johoku, Hamamatsu 432, Japan
(Received 22 November 1994)

This paper presents molecular dynamics simulations of two-dimensional vertically vibrated beds of granules. We have succeeded in observing pressure and density wave propagations that arise from the collective motion of granules. In addition, investigation is made of the variation in kinetic energy per particle along the bed height.

PACS number(s): 46.10.+z, 62.30.+d, 02.70.Ns

The application of vibrations is commonly practiced in industries to achieve certain objectives in powder handling and processing. However, the fundamental physics of particle behavior in vibrated beds, such as convection [1], heap formation [2], and segregation [3], is not fully understood yet. Density fluctuations in the vibrated bed of granular materials can be very large, which may lead to formation of density waves in the bed. In fact, the density wave propagation due to density fluctuations has been observered in x-ray images for the case of granular flow in a hopper [4]. Air pressure profile and pressure wave propagation in vertically vibrated beds of glass beads have been studied by Akiyama *et al.* [5]. Measurements of air pressure at different depths (in the above studies) reveal that the pressure profile depends on the bed height and the phase of the pressure wave shifts with the depth of the particle beds. It has also been confirmed that the total pressure, measured by direct contact of transducers with the granule bed, exhibits similar wave propagation [6]. Measurements of the convection velocity of particles on the vertical sidewalls under reduced pressures in vibrated beds (vibrational frequency 50 Hz, gauge pressure = 0 to −93.3 kPa in beds of 100 mm wide, 30 mm thick, and 60–140 mm high) indicated [7] that the magnitude of reduced air pressure affects the velocity of glass beads smaller than 0.23 mm but not that of glass beads 0.33 mm in mean diameter. Thus simulation studies neglecting the effect of air can be justified for the investigation of granular materials of sufficiently large size.

Discrete numerical simulations of granular materials to date are mainly based on mechanical models where the force interacting between two particles in contact has a linear dependence on the distance between the centers of particles [models based on the distinct element method (DEM)] [8]. We introduce a model of granular materials based on molecular dynamics (MD) simulations, and investigate pressure and density wave propagations in two-dimensional vertically vibrated beds of granules.

The model is based on the postulate that the basic features of granular materials can be described by the excluded volume effect and the dissipation of kinetic energy between the granules. The excluded volume is expressed by a short-range repulsive force $\mathbf{f}_{ij} = -\partial\phi_{ij}/\partial\mathbf{r}_{ij}$ interacting between particles, where ϕ_{ij} takes the form of a discrete short-range repulsive pair potential,

$$\phi_{ij} = \begin{cases} \varepsilon\left[\left(\frac{d}{r_{ij}}\right)^{12} - \left(\frac{d}{r_{ij}}\right)^{6} + \frac{1}{4}\right] & \text{if } |\mathbf{r}_{ij}| < r_0 \\ 0 & \text{otherwise,} \end{cases}$$

where $\mathbf{r}_{ij} = \mathbf{r}_j - \mathbf{r}_i$ and $r_0 = 2^{1/6}d$, d being the characteristic length representing the particle size. The same potential is used to describe the interaction between the particles and the bottom of the container, with $|\mathbf{r}_{ij}|$ being replaced by the distance between the container base and the particles. The normal dissipation force $\mathbf{f}_i = -\gamma m(\mathbf{v}_{ij}\cdot\mathbf{r}_{ij})\mathbf{r}_{ij}/|\mathbf{r}_{ij}|^2$, where γ is the dissipation coefficient and $\mathbf{v}_{ij} = \mathbf{v}_j - \mathbf{v}_i$ is the relative velocity, works for each contact. Gravity and sinusoidal movements of the container are included in the system as external forces. A periodic boundary condition is imposed in the horizontal direction. We use the units of length d, mass m, and energy ε, which make γ the only free parameter in the model. This is significant in that conventional DEM models use two free parameters.

The pair potential ϕ_{ij} has other technical advantages over commonly used potentials since this pair potential diverges at $\mathbf{r}_{ij} \to \mathbf{0}$ and smoothly decays to zero at $|\mathbf{r}_{ij}| = r_0$ while maintaining the discrete nature of the granules, which allows the use of constant-time-step algorithms. Furthermore, the divergence of ϕ_{ij} for $\mathbf{r}_{ij} \to \mathbf{0}$ is effective in preventing unphysical phenomena such as interpenetration of the particles. The model is capable of simulating the bed from very dense to very dilute. The velocity Verlet algorithm is used in this study since no advantage (nor disadvantage except for the lengthy code) seems to exist for using the predictor-corrector algorithm. We use time steps $dt = 1.6\times10^{-4}$, 2.0×10^{-4}, and 2.5×10^{-4} in units of time necessary for one vibrational cycle. The validity check of time steps normally undertaken in MD simulations, such as checking the conservation of energy or tracing back the trajectories by reverse time evolution, cannot be used in dissipative systems. However, the time evolution of the total (potential and kinetic) energy of different time steps reproduces results to within an accuracy of 1% throughout a vibrational cycle for the values of dt we used.

A system consisting of particle number $N = 2000$ in a simulation box with a width of 5 is reported in this study. In smaller systems ($N = 1000$ and 500) having simulation boxes of widths 10 and 5, no artifact in relation to the

 ©1995 The American Physical Society

periodic boundary condition has been detected. We set $\gamma = 0.01g$. Vibrations of amplitude $A = 3.0$ with vibrational acceleration $\Gamma = 3.0g$, where g is the gravitational acceleration, are applied. Snapshots at four phases (a) $\beta = 0$, (b) $\beta = \frac{\pi}{2}$, (c) $\beta = \pi$, and (d) $\beta = \frac{3\pi}{2}$ in the 51st cycle are shown in Fig. 1. The simulation concentrates on how pressure and density waves propagate in the vertical direction; thus the box width is kept at a small value to increase the height of the bed. Each snapshot contains 6.5 simulation boxes. The density change over a vibration cycle can be easily recognized by the difference in the pattern of particle distribution. We can observe stress chains in the area where particles are densely packed. At $\beta = 0$ the vibrational velocity is a maximum in the upward direction, generating a very dense area near the bottom of the container as seen in Fig. 1(a). The dense area moves upward with increasing phase value. No artificial boundary conditions are imposed in the vertical direction, so that the particles are seen to bounce on the top of the bed. For clarity, not all particles bouncing on the top of the bed are shown in the snapshots.

Time profiles of pressure and density over a vibration cycle at bed heights from 7.5 to 147.5 (the average between 145 and 150), equidistantly apart, are shown in Figs. 2 and 3, respectively. The time profiles represent the averaged pressure and density over ten cycles (41st to 50th cycle) in the area 5×5 around a given height. As seen from Fig. 2, the profile near the bottom of the container has a peak near $\beta = 0$, where the upward vibrational velocity is a maximum. The peak shifts towards larger phases with increasing bed height, showing clearly the propagation of a pressure wave. The magnitude of the peak is seen to decrease with increasing bed height as the energy dissipates and density gets smaller. The

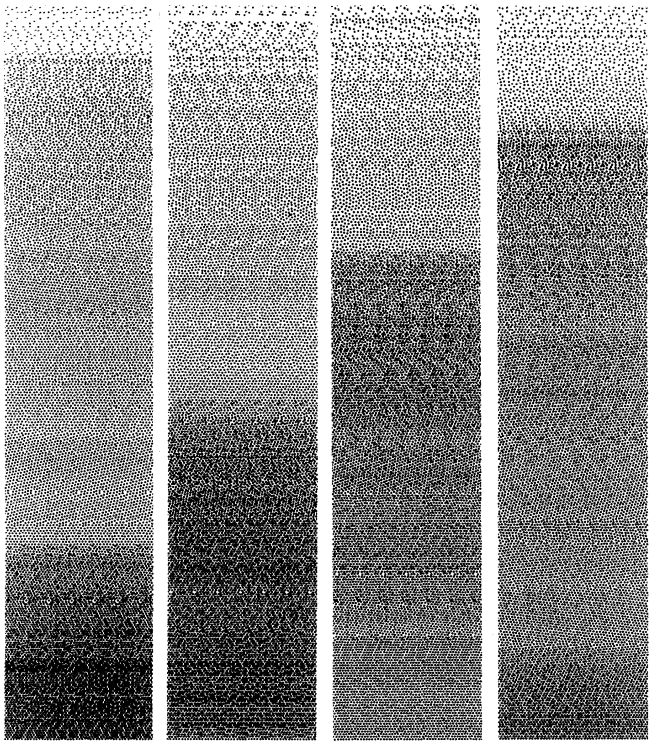

(a) $\beta = 0$ (b) $\beta = \frac{\pi}{2}$ (c) $\beta = \pi$ (d) $\beta = \frac{3\pi}{2}$

FIG. 1. Snapshots of bed at 51st cycle of simulation: respectively at (a) $\beta = 0$, (b) $\beta = \frac{\pi}{2}$, (c) $\beta = \pi$, and (d) $\beta = \frac{3\pi}{2}$.

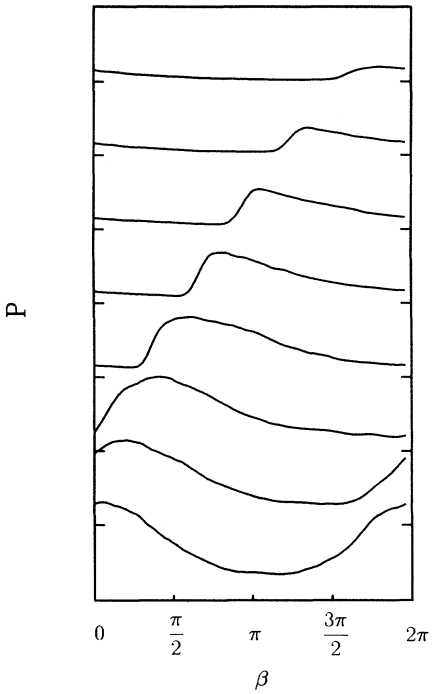

FIG. 2. Time profile of pressure P over one vibration cycle at different heights.

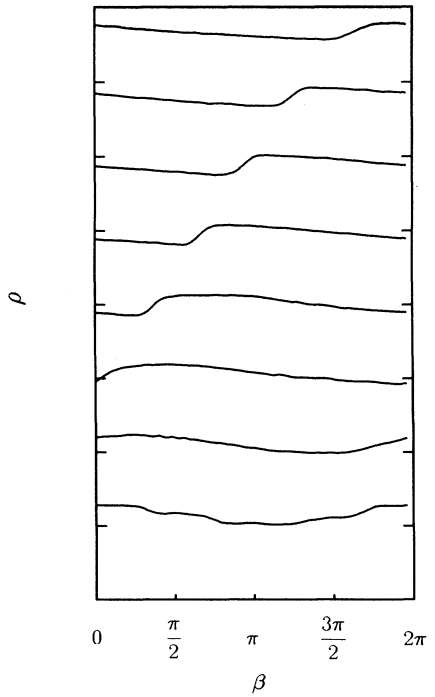

FIG. 3. Time profile of density ρ over one vibration cycle at different heights.

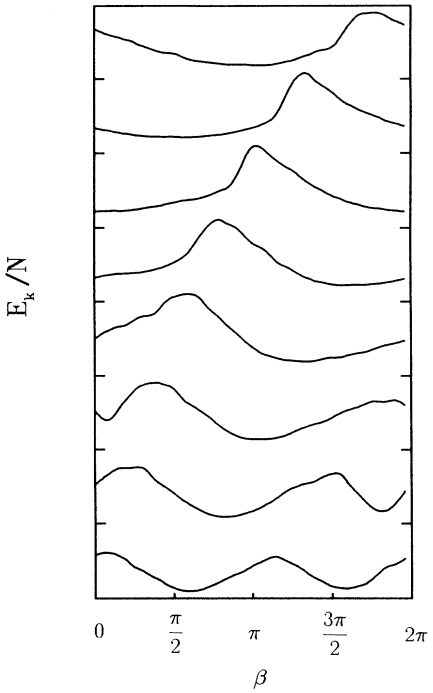

FIG. 4. Time profile of kinetic energy per particle E_k/N over one vibration cycle at different heights.

pressure wave travels half a wave length in a height of approximately 100. In smaller systems the bed height becomes smaller and a phase shift of only less than half a wave length can be observed.

Figure 3 shows that near the bottom of the container the density variation is small over a vibration cycle, maintaining large density values. This contrasts with the corresponding time profile of pressure whose variation over a cycle is quite large. At an intermediate height, a wave front emerges, and the density wave propagates towards the top of the bed in the upper half of the bed.

The fact that clear trends of wave propagation are seen for both pressure and density whose values are averaged ones over ten cycles reflects the collective motion of the granules induced by the vibrational force acting on the bed.

To understand the energy propagation through the bed we show in Fig. 4 the time profile of kinetic energy per particle E_k/N (averaged over ten cycles), at the same bed heights as those for pressure and density. Two peaks can be observed in the energy curve near the bottom of the container, one being near $\beta = 0$, the other near $\beta = \pi$ where the downward velocity is a maximum. Multiple peaks over a cycle appear since the kinetic energy is proportional to the square of the velocity. The two peaks merge at about height 67.5 (the fourth curve from the bottom), which is approximately the height where a clear wave front appears in the density curve. A shift of the peak towards larger phases with increasing bed height can be observed in the upper half of the bed.

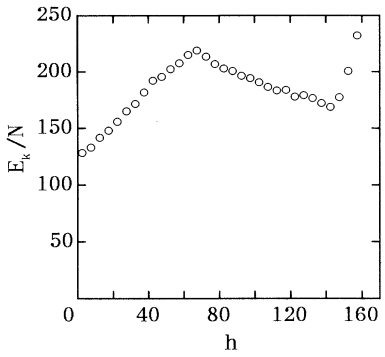

FIG. 5. The relation between kinetic energy per particle E_k/N (ϵ) averaged over ten cycles and bed height h.

The kinetic energy per particle E_k/N (averaged over ten cycles of vibrations for the entire phase) is plotted against the bed height in Fig. 5. The value of E_k/N increases with increasing bed height, peaks at $h \simeq 68$, passes through a minimum at $h \simeq 145$, then increases sharply with h. The explanation for the above behavior of E_k/N is given below. The kinetic energy of particles increases with increasing bed height because particles can move increasingly freely with the decrease in density. However, the dissipation of the energy transmitted to the bed through the vertical vibrations of the container base increases with h. The interplay between the two effects results in a peak at $h \simeq 68$. The drastic increase in the value of E_k/N for height $h \geq 145$ is presumably because the particles are bouncing freely on the top of the bed. This suggests that the local minimum of E_k/N near the top of the bed can be used to define the average bed depth, since a clear-cut bed depth is difficult to define when the condition of the bed surface is continuously changing under vibrations.

We have simulated two-dimensional vertically vibrated beds and succeeded in observing the pressure and density wave propagations through the beds. We have shown that the kinetic energy is dependent not only on the density but also on the bed height because the dissipation of energy transmitted to the bed through the vertical vibrations of the container base increases with the bed height.

[1] C. Laroche, S. Douady, and S. Fauve, J. Phys. (Paris) **50**, 699 (1989); J. Rajchenbach, Europhys. Lett. **16**, 149 (1991); Y.-H. Taguchi, Phys. Rev. Lett. **69**, 1367 (1992); J. A. C. Gallas, H. J. Herrmann, and S. Sokołowski, *ibid.* **69**, 1371 (1992); S. Luding, E. Clément, A. Blumen, J. Rajchenbach, and J. Duran, Phys. Rev. E **50**, R1762 (1994).

[2] P. Evesque and J. Rajchenbach, Phys. Rev. Lett. **62**, 44 (1989); P. Evesque, E. Szmatula, and J.-P. Denis, Europhys. Lett. **12**, 623 (1990); E. Clément, J. Duran, and J. Rajchenbach, Phys. Rev. Lett. **69**, 1189 (1992).

[3] A. Rosato, K. J. Strandburg, F. Prinz, and R. H. Swend-

sen, Phys. Rev. Lett. **58**, 1038 (1987); R. Jullien and P. Meakin, Nature **344**, 425 (1990); J. B. Knight, H. M. Jaeger, and S. R. Nagel, Phys. Rev. Lett. **70**, 3728 (1993).

[4] G. W. Baxter, R. P. Behringer, T. Fagert, and G. A. Johnson, Phys. Rev. Lett. **62**, 2825 (1989).

[5] T. Akiyama, H. Kurimoto, and K. Nakasaki, Chem. Eng. Sci. **44**, 1594 (1989); T. Akiyama, H. Kurimoto, K. Nakasaki, and T. Matsuda, Adv. Powder Technol. **2**, 256 (1991); T. Akiyama, H. Yamaboshi, and T. Matsuda, *ibid.* **4**, 287 (1993); T. Akiyama, H. Yamaboshi, and T. Iguchi, *ibid.* **5**, 43 (1994).

[6] T. Matsuda, MS thesis, Shizuoka University, 1990; the duration of the collision between the bed and the vessel base has also been studied using both the values of total pressure and air pressure by T. Akiyama and H. Kurimoto, Chem. Eng. Sci. **44**, 427 (1989).

[7] T. Akiyama, N. Kimura, and T. Iguchi (unpublished).

[8] P. A. Cundall and O. D. L. Strack, Géotechnique **29**, 47 (1979); O. R. Walton and R. L. Braun, J. Rheol. **30**, 949 (1986); P. K. Haff and T. Werner, Powder Technol. **48**, 239 (1986); P. A. Thompson and G. S. Grest, Phys. Rev. Lett. **67**, 1751 (1991); Y.-H. Taguchi, *ibid.* **69**, 1367 (1992); J. A. C. Gallas, H. J. Herrmann, and S. Sokołowski, *ibid.* **69**, 1371 (1992); T. Pöschel, J. Phys. (France) II **3**, 27 (1993); S. Luding, E. Clément, A. Blumen, J. Rajchenbach, and J. Duran, Phys. Rev. E **50**, R1762 (1994); J. Lee, J. Phys. A **27**, L257 (1994).